PRAMANA
— journal of
physics

Vol. 77, No. 5
November 2011
pp. 793–802

Classically induced suppression of energy growth in a chaotic quantum system

HARINDER PAL[1] and M S SANTHANAM[2,*]

[1]Physical Research Laboratory, Navrangpura, Ahmedabad 380 009, India
[2]Indian Institute of Science Education and Research, Pashan Road, Pune 411 008, India
*Corresponding author. E-mail: santh@iiserpune.ac.in

Abstract. Recent experiments with Bose–Einstein condensates (BEC) in traps and speckle potentials have explored the dynamical regime in which the evolving BEC clouds localize due to the influence of classical dynamics. The growth of their mean energy is effectively arrested. This is in contrast with the well-known localization phenomena that originate due to quantum interferences. We show that classically induced localization can also be obtained in a classically chaotic, non-interacting system. In this work, we study the classical and quantum dynamics of non-interacting particles in a double-barrier structure. This is essentially a non-KAM system and, depending on the parameters, can display chaotic dynamics inside the finite well between the barriers. However, for the same set of parameters, it can display nearly regular dynamics above the barriers. We exploit this combination of two qualitatively different classical dynamical features to obtain saturation of energy growth. In the semiclassical regime, this classical mechanism strongly influences the quantum behaviour of the system.

Keywords. Non-Kolmogorov–Arnold–Moser chaos; quantum chaos; localization.

PACS Nos 05.45.Mt; 68.65.Fg; 05.45.Pq

1. Introduction

One of the significant results in the field of quantum chaos is the discovery of dynamical localization [1]. This refers to the saturation of temporal energy growth, originally studied in the quantum kicked rotor, due to quantum interferences. Soon it was established that dynamical localization is analogous to the well-known Anderson localization [1]. Though Anderson localization was originally proposed with respect to the dynamics of electrons in a crystalline lattice [2] with random potentials, over the years it has been realized that it is a more general effect that appears in many other contexts as well [3]. In 1994, dynamical localization was experimentally realized in the laboratory using cold atoms in optical lattices [4]. In some systems, in contrast with this dynamical localization, it is also possible to realize localization that is essentially influenced by classical dynamics. In such cases, it is important to be able to distinguish between classically induced saturation of energy growth and the quantum localization effects. In the last few years,

DOI: 10.1007/s12043-011-0190-4; ***e*Publication: 22 October 2011**

there were a series of experiments with BECs evolving in finite box and optical speckle-type potentials which displayed suppression of energy growth due to classical mechanism [5]. In these experiments, contrary to the expected localization due to quantum effects, the observed suppression of energy growth could be explained by purely classical mechanism in which energy exchange between the particles played a vital role. The question then is if the non-interacting particles in chaotic systems can display this phenomenon in a non-trivial manner. This would lead to a better understanding of the physics behind the interplay between interactions and localization. The purpose of this article is two-fold: (1) to study the classical and quantum dynamics of a chaotic system in which the periodically kicked particles evolve from a confined region of the potential, (2) to show that the energy growth of these evolving particles, under certain circumstances, is suppressed. This system does not obey the Kolmogorov–Arnold–Moser (KAM) theorem [6]. In addition, the momentum-dependent boundary conditions due to finite potential barriers lead to a richer variety of classical dynamical features. The suppression of energy growth is effected by the presence of both the KAM-like and non-KAM classical structures in phase space. To the best of our knowledge, there are not many examples of such systems which display characteristics of both KAM-type and non-KAM-type classical dynamics.

2. Model system

We consider the dynamics of a non-interacting particle initially located inside a finite potential well constructed by placing two potential barriers each of height V_0 and width b kept $x_r - x_l$ apart (see figure 1). Here, x_l and x_r are the left and right inner boundaries of the double-barrier potential, respectively. The particle is further subjected to periodic δ-kicks generated by a spatially periodic potential field of wavelength λ. We can scale the coordinate system to obtain the dimensionless Hamiltonian as

$$H = \frac{p^2}{2} + V_{sq}(x) + \epsilon \cos(x) \sum_{n=-\infty}^{\infty} \delta(t - n). \tag{1}$$

Since λ, m, T do not appear as independent parameters in the scaled Hamiltonian, we also fix $\lambda = 2\pi$, $m = 1$ and $T = 1$. With this choice, the stationary potential term in eq. (1) becomes $V_{sq}(x) = V_0 [\Theta(x - x_l + b) - \Theta(x - x_l) + \Theta(x - x_r) - \Theta(x - x_r - b)]$. Amplitude ϵ of the kicking field is generally referred to as kick strength. The classical dynamics

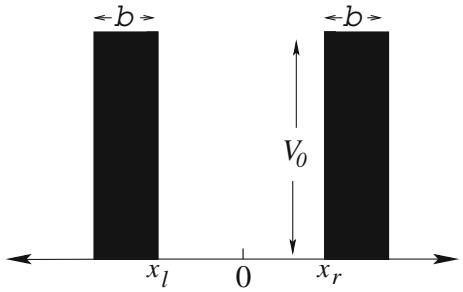

Figure 1. The schematic of the potential V_{sq}.

depends on the positions $\mathbf{B} = \{x_l - b, x_l, x_r, x_r + b\}$ of the boundaries of double-barrier structure, the kick strength ϵ and the potential height V_0. Dynamics of particles in double barrier structures can be experimentally realized in the laboratory [7]. We investigate the model keeping in view its possible experimental realization as well.

3. Classical dynamics

The Hamiltonian in eq. (1) is classically integrable for $\epsilon = 0$. For $\epsilon > 0$, the system is non-integrable and, except for some particular choices of parameters, displays mixed phase space. For convenience, we can write down the Hamiltonian in eq. (1) as

$$H = H_0 + V_{sq}, \tag{2}$$

where $H_0 = (p^2/2) + \epsilon \cos(x) \sum_{n=-\infty}^{\infty} \delta(t - n)$ represents the standard kicked rotor Hamiltonian that leads to the standard map [8]. Thus, the system is equivalent to a kicked rotor subjected to the stationary potential V_{sq}. The dynamics of H is mainly governed by that of H_0 in addition to being subjected to the discontinuities in V_{sq} which are incorporated through appropriate boundary conditions [9]. Going by this approach, we obtain the following map:

$$p_n = p_{n-1} + \epsilon \sin(x_{n-1}), \quad x_n = x_{n-1} + p_n, \tag{3a}$$

$$\begin{pmatrix} p_n \\ x_n \end{pmatrix} \to \hat{\mathcal{R}} \begin{pmatrix} p_n \\ x_n \end{pmatrix}. \tag{3b}$$

Equation (3a) represents the effect of H_0 and is identical to the standard map defined on $x, p \in [-\infty, \infty]$. In eq. (3b), the operator $\hat{\mathcal{R}} = \hat{\mathcal{R}}_k \ldots \hat{\mathcal{R}}_2 \hat{\mathcal{R}}_1$ represents the effect due to k encounters of the particle, between two kicks, with the discontinuities of V_{sq} at positions represented by $B_1, B_2, \ldots, B_k$ respectively. Depending on energy E of the particle being $E > V_0$ or $E < V_0$, each of these k encounters could either be a reflection (sign of the momentum changes) or refraction (magnitude of the momentum changes) at $B_i \in \mathbf{B}$, $i = 1, 2, ..., k$. The explicit forms for the operators $\hat{\mathcal{R}}_i$ can be obtained from [9] and we do not pursue that in this paper.

In the simulations presented here, we have taken the position of barriers to be symmetric about 0, i.e., $x_l = -x_w$ and $x_r = x_w$. In figure 2 we show the stroboscopic Poincaré section for two choices of parameters with initial conditions uniformly distributed in the region in $x \in (-x_w, x_w)$, $p \in (-p_c, p_c)$, where $p_c = \sqrt{2mV_0}$ is the minimum momentum required for the particle to cross the barrier. We refer to this region with x in $(-x_w, x_w)$ as the well region. The major feature we notice in figures 2a and 2b is the absence of invariant curves. This differs strongly from the standard map dynamics which shows quasiperiodic orbits for such low kick strengths. This behaviour in the dynamics of H is due to the non-KAM nature of the system. This can be explained as follows. Clearly, when a particle evolves between two successive encounters with the boundaries of $V_{sq}(x)$, it follows a trajectory that is identical with one of the quasiperiodic orbits of the corresponding standard map (defined with $V_0 = 0$ in eq. (1)). Due to the discontinuous potential $V_{sq}(x)$, the particle would break away from one such quasiperiodic orbit to join another at each encounter with the boundary. This leads to the breaking of quasiperiodic orbits and development of mixed

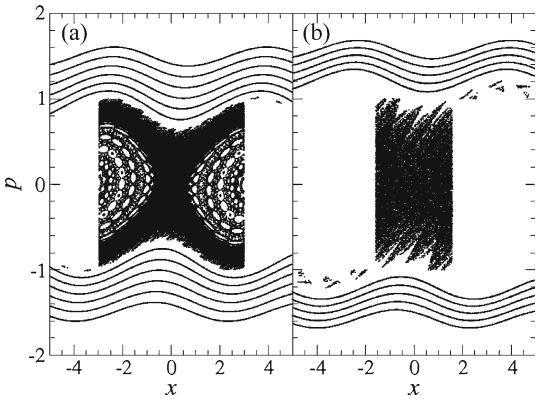

Figure 2. Stroboscopic Poincaré section for the Hamiltonian in eq. (1) for $b = 0$, $\epsilon = 0.15$, $V_0 = 0.5$. In (**a**) $x_w = 0.95\pi$ and (**b**) $x_w = 0.5\pi$.

phase space comprising intricate chains of islands embedded in the chaotic sea. From a theoretical perspective, the non-KAM nature of the system can be attributed to non-analytic $V_{sq}(x)$ which violates the assumptions of KAM theorem [6]. In such a non-KAM system, one can obtain chaotic dynamics even when the control parameter ϵ is tuned infinitesimally away from its integrable limit. A related model that displays similar non-KAM features is the kicked particle in an infinite potential well whose classical and quantum dynamics are reported in [10].

Figures 2a and 2b also show some of the invariant curves. A particle escaping from the well will encounter the discontinuous $V_{sq}(x)$ only twice, once at each of the inner and outer edges of the barrier it is crossing. Suppose a particle follows a quasiperiodic orbit $C_1(\mu_1)$ with winding number μ_1 before it encounters the boundary at x_w and, emerges out in the region $x > x_w + b$ on an orbit $C_2(\mu_2)$ with winding number μ_2. It can be shown that as $b \to 0$, $\mu_1 \to \mu_2$ [9]. In this situation, trajectories of the particles crossing the double-barrier structure without suffering any reflection resemble the invariant tori of the corresponding standard map. This leads to KAM-like behaviour in a non-KAM system. For $b > 0$, the trajectory of a particle is discontinuous at the barrier edges and $C_1(\mu_1)$ and $C_2(\mu_2)$ are well separated. However, due to the absence of multiple encounters with discontinuities in the well region, the system continues to exhibit regular behaviour like a KAM system. This is contrary to the general behaviour of non-KAM systems in which such breakdown of invariant tori leads to a mixed phase space comprising chaotic region and dense set of islands. Hence, we call this behaviour also as a KAM-like behaviour. For $\epsilon \ll 1$, thus, the phase space can be broadly divided into two regions. One of these shows typical non-KAM features, i.e. mixed phase space even for small values of kick strength and the other one shows KAM-like dynamics. For x_w less than the wavelength λ of the kicking field, most of the islands in the mixed phase space accumulate near the inner boundaries of the double-barrier structure (see figure 2a). This allows the chaotic particles to travel to high momentum regions and leads them to KAM-like (non-diffusive) region of phase space. The results to be presented in §5 are based on this coexistence of non-KAM and KAM-like phase space features.

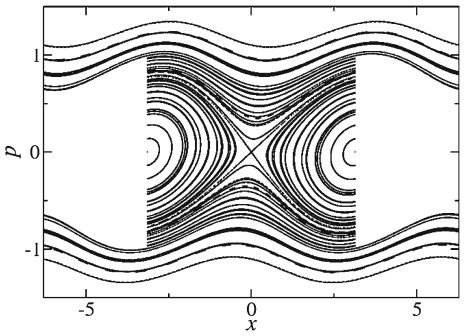

Figure 3. Stroboscopic Poincaré section for the Hamiltonian in eq. (1) for $b = 0$, $\epsilon = 0.15$, $V_0 = 0.5$, $x_w = \pi$.

Another interesting feature of classical phase space can be seen only for special choices of parameters, namely, the KAM-like behaviour even for particles that undergo multiple reflections, i.e., in the well region that would otherwise have chaos and islands (see figure 2a). This is observed if the condition $x_w = \pm(l\lambda/2)$, l being an integer, is satisfied. This happens through the following mechanism: As pointed out earlier, between successive reflections from the barriers, the particle follows a quasiperiodic orbit. It has also been mentioned that these reflections taking place repeatedly lead to breaking of dynamics away from these quasiperiodic orbits. However, when this condition is satisfied, the reflections make the particle hop between a pair of quasiperiodic orbits which have momenta differing only by a sign. This pair of two quasiperiodic orbits acts like an overall new quasiperiodic orbit. As a result, we see only quasiperiodic orbits as shown in figure 3.

4. Quantum dynamics

The time-dependent Schroedinger equation corresponding to the scaled Hamiltonian in eq. (1) is given by

$$i\hbar_s \frac{\partial \psi}{\partial t} = \left[\frac{-\hbar_s^2}{2} \frac{\partial^2}{\partial x^2} + V_{sq}(x) + \epsilon \cos x \sum_n \delta(t-n) \right] \psi, \tag{4}$$

where $\hbar_s$ is the scaled Planck's constant. This being a periodically kicked system, we can obtain the one-period Floquet operator,

$$\hat{U} = \exp\left(-\frac{i\epsilon}{\hbar_s} \cos x \right) \exp\left(-\frac{i}{\hbar_s} \left[\frac{p^2}{2m} + V_{sq} \right] \right), \tag{5}$$

such that $\psi(x, n) = \hat{U}^n \psi(x, 0)$. The classical limit will correspond to taking $\hbar_s \to 0$.

We choose the parameters $\hbar_s$ and width of the barrier b such that we stay in the semiclassical regime and tunnelling is largely suppressed. To perform the quantum simulations of this system, we evolve an arbitrary wave packet $\psi(x, n = 0)$ confined initially between the barriers, such that $\psi(x, n) = \hat{U}^n \psi(x, n = 0)$. In practice, we have solved the time-dependent Schroedinger equation using a split-operator method in conjunction with the fast Fourier transform to go from position to momentum representation and

vice versa. In our calculations, a typical step size on time axis is $O(10^{-3})$ and the spatial step size is $O(10^{-4})$ such that the evolved wave packets converged to at least six decimal places. We compute the Husimi distribution [11] (not shown here) defined by $Q(x_0, p_0, n) = |\langle\psi(x, n)|x_0, p_0\rangle|^2$ where we have taken $\langle x|x_0, p_0\rangle$ as the minimum uncertainty wave packet. In the semiclassical regime, as the Husimi distribution reveals, the quantum dynamics resembles the classical dynamics.

5. Saturation of energy growth

In this section, we show that, if $\epsilon < 1$, the presence of both the KAM-type and non-KAM type classical dynamical structures in the phase space leads to saturation of the mean energy of the system [9]. Though the complete arrest of energy growth can occur only as $n \to \infty$, the time at which the energy growth effectively saturates is finite when measured in the units of T. In the semiclassical regime, as $\hbar_s \to 0$, this classical effect dominates the quantum behaviour as well. This 'classical localization effect' must be distinguished from the localization effect induced by quantum coherences.

To understand the classical origin of this effect, we refer to the Poincaré section shown in figure 4 which shows full chaos, to resolution of our calculation, in the well region. As the kicks begin to act, any localized distribution $\rho(x, p; n = 0)$ of the initial conditions will be quickly dispersed by the chaotic dynamics. This also ensures that $\langle E\rangle_s$ will be independent of the particular choice of initial conditions. As the kicks impart energy to the system, some of the particles with $|p| > p_c$ will escape from the well region. Since the dynamics between successive kicks follows that of the kicked rotor, we discuss the escape mechanism in terms of the invariant curves of the corresponding kicked rotor ($V_0 = 0$ in eq. (1)). In figure 4, we identify invariant curves $C_\pm(\mu_b)$ and $C_\pm(\mu_c)$, μ_b and μ_c being

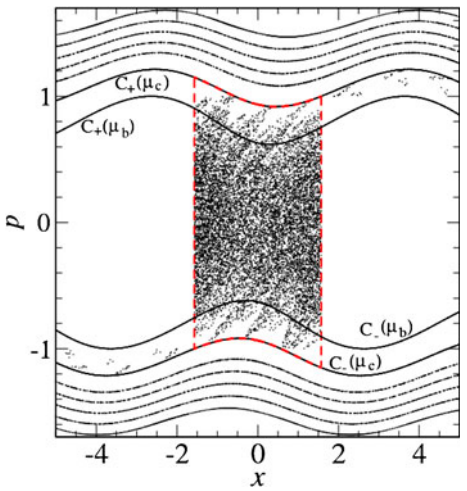

Figure 4. The stroboscopic Poincaré section for $b = 0, \epsilon = 0.15, V_0 = 0.5$ and $x_w = 0.5\pi$.

their winding numbers. The invariant curves $C_+(\mu_b)$ and $C_-(\mu_b)$ are defined such that the maximum value of $|p|$ is equal to p_c. This implies that all the invariant curves with winding number $\mu < \mu_b$ will have $|p| < p_c$ and hence the particles on them will necessarily get reflected at the barrier obstructing their escape from the well region. In a similar vein, the invariant curves $C_+(\mu_c)$ and $C_-(\mu_c)$ are defined such that the particles with $\mu > \mu_c$ will never undergo reflection and, thus, will surely escape from the well region. This is shown as red curve in the figure. However, if a particle has winding number $\mu_b < \mu < \mu_c$, then particle might or might not escape.

To escape out of the well region, every phase space point in the chaotic layer must first reach any of the invariant curves $C(\mu)$ with $\mu_b < \mu < \mu_c$. As $n \to \infty$, in the chaotic regime, all the particles absorb sufficient energy from the kicking field and will ultimately leave the well region. The escaped particles get locked on to invariant curves $C(\mu)$ of the corresponding standard map. As $n \to \infty$, this leads to the momenta of particles leaving the well region settling on to a time-independent distribution on the invariant curves $C(\mu)$ with $\mu_b < \mu < \mu_c$. This leads to energy growth being arrested. In figures 5b and 5c, the classical ($f_n(p)$) and quantum ($F_n(p) = |\tilde{\psi}(p)|^2$) momentum distributions are plotted for $n = 250$ and 300. The classically induced localization is seen in the nearly invariant momentum distributions for $n > 250$.

The mean saturated energy $\langle E \rangle_s$ will be formally $\langle p^2/2 \rangle$ where the average is over the invariant curves with $\mu_b < \mu < \mu_c$. This is often not straightforward to compute. Hence, in figure 5a, we show the numerically obtained mean saturated energy $\langle E \rangle_s$ as dot-dashed line. Further, we note that it takes only finite time (order of a few hundred kicks) for the particle density inside the well to become vanishingly small though it will become zero only as $n \to \infty$. As a result, the mean energy nearly saturates to $\langle E \rangle_s$ in finite time (see figure 5a).

In the semiclassical regime, the quantum dynamics behaves in an analogous manner. The quantum mean energy can be calculated as

$$\langle E \rangle_n = \frac{1}{2} \int_{-\infty}^{\infty} \tilde{\psi}(p, n) p^2 \, \tilde{\psi}(p, n) \, \mathrm{d}p. \tag{6}$$

This is shown as dotted line in figure 5a and this too nearly saturates at finite time. Note that the discrepancy between the classical and quantum mean is a reminder that the effective Planck's constant is such that the system is not entirely in the semiclassical regime.

We remark that for energy growth saturation, complete chaos between the barriers is not essential. However, in case of mixed phase space between the barriers, $\langle E \rangle_s$ will depend upon the initial state. If some islands are present, then the fraction of the particles having initial states on one of these islands would be trapped inside forever and, thus, $\langle E \rangle_s$ will be the weighted average energy of the trapped and escaped particles. Also, due to the sticky nature of these islands, even the chaotic particles will take longer to escape from the double-barrier structure leading to increase in time required for saturation. Finally, we note that a kind of energy growth suppression is known to occur in the classical kicked rotor for certain choice of kick strengths. This sub-diffusion phenomenon happens due to the presence of sticky islands embedded in the phase space. But this does not, in general, lead to classical or quantum steady states. In contrast to this, the dynamics of Hamiltonian in eq. (1) leads to saturation of energy growth and steady states through a mechanism that does not depend upon sticky islands.

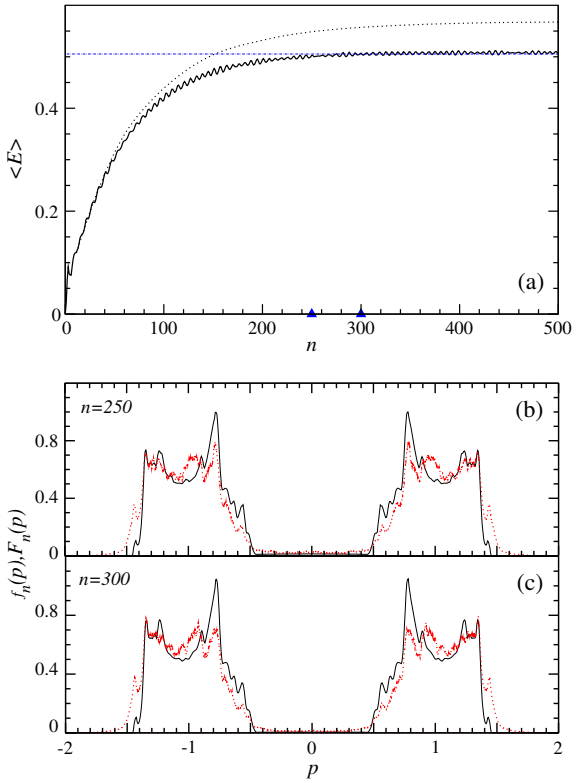

Figure 5. (**a**) The classical (solid line) and quantum (dotted line) mean energies as a function of integer time n. In (**a**), the horizontal line in blue is the numerically estimated average $\langle E\rangle_s$ for the classical system. Note that for the classical system, the mean energy $\langle E\rangle$ almost saturates to $\langle E\rangle_s$ at $n = 250$. In (**b**) and (**c**), the classical and quantum momentum distributions are shown for $n = 250$ and 300 (marked as triangles in (**a**)). The parameters used are: $b = 0.1$, $\epsilon = 0.3$, $V_0 = 0.5$ and $x_w = 0.5\pi$. For quantum calculation, $\hbar_s = 0.0025$.

5.1 *Behaviour for large kick strengths*

In §5, we showed evidence for suppression of energy growth leading to steady states for low kick strengths, $\epsilon < 1$. In this section, we show that the classical dynamics of our system in eq. (1) displays nearly normal diffusion corresponding to unbounded growth of energy for large kick strengths, i.e., $\epsilon \gg 1$. This behaviour is similar to the classical dynamics of the standard kicked rotor. This normal diffusion for $\epsilon \gg 1$ can be explained as follows. Note that for $\epsilon < 1$ we had emphasized the role played by non-KAM and KAM-like classical structures in bringing about energy saturation. However, if the kick strength $\epsilon \gg 1$, then most of the invariant curves in the region of KAM-like behaviour are also destroyed and the chaos dominates throughout the phase space. In such a scenario, the energy growth is not arrested and, instead, we obtain the diffusive energy growth regime similar to the one that would be seen in kicked rotor at the same value of kick strengths. This is shown in

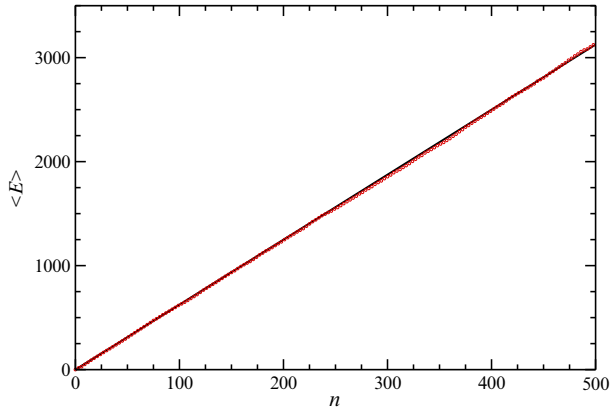

Figure 6. Growth in mean energy (open circles, red) as a function of time n for kick strength $\epsilon = 5$ obtained from simulations. The other parameters are the same as in figure 5a. The black solid line corresponds to the analytical result $\langle E\rangle = (\epsilon^2/4)n$ for the kicked rotor.

figure 6 with $\epsilon = 5$. For the classical kicked rotor, energy growth is $\langle E\rangle = (\epsilon^2/4)n$ [8]. This estimate is also consistent with the energy growth in the system in eq. (1) for $\epsilon \gg 1$. Hence, for large kick strengths, our model in eq. (1) behaves like a kicked rotor at the same kick strengths. Then, the role of finite barriers becomes insignificant and classical suppression of diffusion is not observed.

6. Summary and conclusions

As pointed out earlier, several experiments in recent times have attempted to explore a scenario for the arrest of energy growth or 'localization' that is induced by classical structures. These experiments have largely focussed on Bose–Einstein condensates along with their interparticle interactions. We have chosen to study if a similar scenario can be realized in a classically chaotic system with non-interacting particles which turns out to be a non-KAM system as well. This can be thought of as one possible generalization of the kicked rotor that includes a stationary potential. In addition, as we pointed out before, this can also be experimentally realized in a laboratory. One surprising feature of the system is that even though it is non-KAM, it exhibits KAM-like dynamics in most part of its phase space. We exploit the existence of a diffusive phase space region immersed in a non-diffusive one due to interplay between non-KAM and KAM-like dynamics to obtain one possible scenario for the saturation of energy growth in a chaotic system with non-interacting particles. In the semiclassical regime, this mechanism carries over to the quantum domain as well. Thus, in the quantum domain, we obtain 'localization' that can be explained on the basis of classical dynamical structures in phase space. In this sense, this is similar in spirit to the scarring effect, an enhanced quantum probability density in the vicinity of classical periodic orbits, widely studied in time-independent chaotic systems such as the coupled quartic oscillator and atoms in strong magnetic fields [12]. Finally, we remark that in the last few years, there is considerable interest in the field of chaotic ratchets [13]. By appropriately breaking

spatio-temporal symmetries, this system can provide new ways of exploiting non-KAM type classical dynamics for obtaining directed transport in a chaotic system.

Acknowledgements

The quantum calculations for this work was done on the HP cluster computer at PRL, Ahmedabad, India.

References

[1] G Casati, B V Chirikov, F M Izrailev and J Ford, *Lect. Notes Phys.* **93**, 334 (1979)
S Fishman, D R Grempel and R E Prange, *Phys. Rev. Lett.* **49**, 509 (1982)
[2] P W Anderson, *Phys. Rev.* **109**, 1492 (1958)
[3] A Lagendijk, B van Tiggelen and D S Wiersma, *Phys. Today* **62**, 8 (2009)
A Aspect and M Inguscio, *Phys. Today* **62**, 8 (2009)
[4] F L Moore *et al*, *Phys. Rev. Lett.* **73**, 2974 (1994)
F L Moore *et al*, *Phys. Rev. Lett.* **75**, 4598 (1995)
[5] K Henderson *et al*, *Europhys. Lett.* **75**, 392 (2006)
D Clement *et al*, *Phys. Rev. Lett.* **95**, 170409 (2005)
C Fort *et al*, *Phys. Rev. Lett.* **95**, 170410 (2005)
T Schulte *et al*, *Phys. Rev. Lett.* **95**, 170411 (2005)
L Sanchez-Palencia *et al*, *New J. Phys.* **10**, 045019 (2008)
[6] Michael Tabor, *Chaos and integrability in nonlinear dynamics: An introduction* (Wiley-Interscience, 1989)
[7] G Jona-Lasinio, C Presilla and F Capasso, *Phys. Rev. Lett.* **68**, 2269 (1992)
C Presilla, G Jona-Lasinio and F Capasso, *Phys. Rev.* **B43**, 5200(R) (1991)
A J McNary and A Puri, *J. Appl. Phys.* **80**, 247 (1996)
[8] L E Reichl, *The transition to chaos: Conservative classical systems and quantum manifestations* (Springer, New York, 2004)
[9] Harinder Pal and M S Santhanam, *Phys. Rev.* **E82**, 056212 (2010)
[10] R Sankaranarayanan, A Lakshminarayan and V B Sheorey, *Phys. Rev.* **E64**, 046210 (2001); *Phys. Lett.* **A279**, 313 (2001)
B Hu *et al*, *Phys. Rev. Lett.* **82**, 4224 (1999)
[11] K Takahashi and N Saiton, *Phys. Rev. Lett.* **55**, 645 (1985)
[12] E J Heller, *Phys. Rev. Lett.* **53**, 1515 (1984)
M S Santhanam, A Lakshminarayan and V B Sheorey, *Phys. Rev.* **E57**, 345 (1998)
K Muller and D Wintgen, *J. Phys. B: At. Mol. Opt. Phys.* **27**, 2693 (1994)
[13] T Salger *et al*, *Science* **326**, 1241 (2009)
A Kenfack, J Gong and A K Pattanayak, *Phys. Rev. Lett.* **100**, 044104 (2008)
S Flach *et al*, *Phys. Rev. Lett.* **84**, 2358 (2000)
H Schanz *et al*, *Phys. Rev. Lett.* **87**, 070601 (2001)
T S Monteiro *et al*, *Phys. Rev. Lett.* **89**, 194102 (2002)
E Lundh and M Willin, *Phys. Rev. Lett.* **94**, 110603 (2005)
J Gong and P Brumer, *Phys. Rev. Lett.* **97**, 240602 (2006)